Surface, interfaces and phase transitions in Al-In monotectic alloys

I. Kaban, S. Curiotto, D. Chatain, W. Hoyer

Available online at www.sciencedirect.com
ScienceDirect
Acta Materialia 58 (2010) 3406–3414
Acta MATERIALIA
www.elsevier.com/locate/actamat

Surfaces, interfaces and phase transitions in Al–In monotectic alloys

I. Kaban [a,*], S. Curiotto [b], D. Chatain [b], W. Hoyer [a]

[a] Institute of Physics, Chemnitz University of Technology, D-09107 Chemnitz, Germany
[b] CNRS, Aix-Marseille Université, CINAM-UPR3118, Campus de Luminy, Case 913, 13288 Marseille cedex 09, France

Received 9 January 2010; received in revised form 5 February 2010; accepted 7 February 2010
Available online 11 March 2010

Abstract

Surface and bulk liquid phase transitions are measured by a unique method currently used to determine surface and interfacial tension of liquid alloys. Focusing on the Al–In system, the location of the liquid miscibility gap was determined from the critical to the monotectic temperatures. The surface tensions of nine liquid alloys, the interfacial tension between coexisting liquids and their densities were measured as a function of temperature. Implementing the bulk data extracted from the asymmetric miscibility gap into a sub-regular model reproduced the experimental surface and interfacial tensions. The wetting temperature was estimated to lie well below the monotectic temperature. The micrometer thickness of the In-rich films which wet the surface of the Al-rich liquid phase after solidification is suggested to be due to the growth of the equilibrium wetting film by diffusion from the Al-rich phase during cooling.

Keywords: Al–In; Monotectic; Complete wetting; Surface transition; Density

1. Introduction

Knowledge of interfacial phenomena and wetting in monotectic alloys is particularly important for engineering multiphase composites, often synthesized by directional solidification [1,2]. Such alloys are promising in many fields extending from the advanced self-lubricating bearings up to superconductors. Density, liquid surface tension (ST), liquid–liquid (*l–l*) interfacial tension (IFT) and their temperature dependence are among the important physical parameters that determine the nucleation rate [2,3] and the thermocapillary (Marangoni) motion [2,4] of the droplets nucleated during cooling within the miscibility gap.

We are interested in the collection of consistent bulk, surface and interfacial data in the Al–In system and their connection through a thermodynamic modelling. Few of these data are available and there is no computational approach where bulk, surface and interfacial data are consistent. The first attempt to determine (*l–l*) IFT in the Al–In system was made by Martin-Garin et al. [5] in 1981. In 1996, it was measured in a wide temperature range by Merkwitz [6,7]. The ST of some liquid Al–In alloys of low In content was determined by Lang [8] and Alchagirov et al. [9]. And, to our knowledge, there are no data on the density of Al–In alloys.

Alloys with a liquid miscibility gap undergo wetting transitions which play an essential role in the microstructure of monotectic alloys. In 1977, Cahn [10] showed theoretically that a transition from partial to complete wetting (wetting transition) should occur in two-phase liquid systems at some temperature T_W below the critical temperature T_C. Above this temperature, at coexistence, one of the liquids intrudes as a film at the surface of the other liquid and/or at its interface with a wall (i.e. a crucible). The wetting temperature, T_W, above which the wetting film is stable, depends on the properties of immiscible system and on the external phase (gas or solid). This wetting phenomenon was first demonstrated to occur in organic mixtures [11] and later in Ga-based immiscible alloys (see for example [12,13]). In some organic mixtures (e.g. methanol–cyclohexane–water)

* Corresponding author. Present address: IFW Dresden, Institute for Complex Materials, P.O. Box 270116, D-01171 Dresden, Germany. Tel.: +49 351 4659 698; fax: +49 351 4659 452.
E-mail addresses: ivan.kaban@physik.tu-chemnitz.de; i.kaban@ifw-dresden.de (I. Kaban).

1359-6454/$36.00 © 2010 Acta Materialia Inc. Published by Elsevier Ltd. All rights reserved.
doi:10.1016/j.actamat.2010.02.015

complete wetting takes place close to the critical temperature, while in other ones (methanol–cyclohexane) it has been observed to stand in the whole range of temperature where the liquid gap is stable [11]. In Ga-based monotectic alloys complete wetting has also been detected over the whole miscibility gap. The wetting transition was found well below the eutectic temperature for the Ga–Pb [14], Ga–Tl [15] and Ga–Pb–Tl [16] systems, and somewhere below the monotectic temperature in Ga–Bi [17]. Such a low wetting temperature has been suggested to be related to the high surface tension values of metallic liquids as compared to those found for organic liquid [18]. A wetting temperature below the monotectic temperature is not a peculiarity of Ga-based alloys, but also stands in Al-based alloys [6,19]. After solidification of $Al_{80.3}Bi_{19.7}$ (at.%) sample, the Al-rich phase was found to be covered by a rather regular Bi-rich layer of a thickness between 8 and 125 μm [19]. While in the paper of Moldover and Cahn [11] the thickness of the wetting layer is not given, it is noted that it is macroscopically thick. However, far from the critical temperature, both theories and experiments performed in organic liquids conclude that the wetting layer cannot be larger than a few tens of nanometers [20]; this is only in the vicinity of T_C that micron size thickness wetting layer could theoretically exist [21].

In this paper we present the first complete study of surface and bulk phase transitions in the Al–In monotectic system. We demonstrate that the liquid–liquid phase separation can be detected by tensiometry and that the acquired data allow redrawing a more precise miscibility gap, in particular in the vicinity of the critical point. We report measurements of the surface tension of Al–In liquid alloys in the single-phase domain, and of the (*l*–*l*) interfacial tension over the whole miscibility gap. We show that, in the Al–In system, complete wetting stands above and below the monotectic temperature. We also discuss the meaning of the thickness of the wetting film observed after solidification of Al–In two-phase alloys. The thermodynamic data extracted from the assessed miscibility gap are used to calculate the surface and interfacial energies with a sub-regular multilayer model [22]. This model is also used to estimate the wetting temperature in the metastable range of the liquid miscibility gap.

2. Experimental

We briefly summarize the method used to measure the surface tension and the interfacial tension of our liquid alloys; the details are given elsewhere [6,7,19,23,24]. The experimental technique is based on the Wilhelmy method that measures the weight of a meniscus attached to a plate [25]. We measure the variation of the weight P of an alumina cylindrical stamp as a function of its immersion depth h when it is pushed in and pulled out of a liquid phase through a liquid–vapor or a liquid–liquid interface. The weight of the stamp $P(h)$ varies due to the changes in buoyancy and capillary forces.

The buoyancy force is directly proportional to the density of the liquid phase in which the stamp is immersed, and to the depth of immersion. When the stamp is immersed into the denser liquid, below the level of the (*l*–*l*) interface, the buoyancy force becomes proportional to the density difference between the two liquids.

The capillary phenomena are described by the Laplace–Young equation of capillarity [26,27]. The capillary force is proportional to the perimeter of the cylinder on which a meniscus is attached, to the ST or the IFT, and to the cosine of the contact angle of the meniscus on the cylinder. On the other hand, the capillary force is equal to the weight of liquid displaced by the meniscus [28,29]. The relationship between the shape of the meniscus (Laplace–Young equation) and the capillary force exerted by the meniscus on the stamp (measured experimentally) underlies the basis for the determination of the surface and interfacial tension [6,7,19,23,24].

An example of a $P(h)$ curve acquired for a two-phase $Al_{64}In_{36}$ alloy close to the monotectic temperature is shown in Fig. 1 (here and hereafter compositions of the Al–In alloys are given in at.%). The ST of the less dense liquid (Al-rich) can be determined from the experimental data measured when the stamp is in the vicinity of the surface (stages S1–S5), and the IFT can be determined from the data obtained when the stamp is in the vicinity of the (*l*–*l*) interface (stages IF4–IF7). From the linear parts of the experimental curve (stages S3–S4 and IF3–IF4) the density of Al-rich and In-rich liquids can be extracted. Details are given elsewhere [6,23,30].

Fig. 2 presents a series of weight-immersion depth curves measured after the point IF1 at different temperatures in the $Al_{75}In_{25}$ alloy. When acquired below the binodal temperature of this alloy (<1088 K) where two liquids

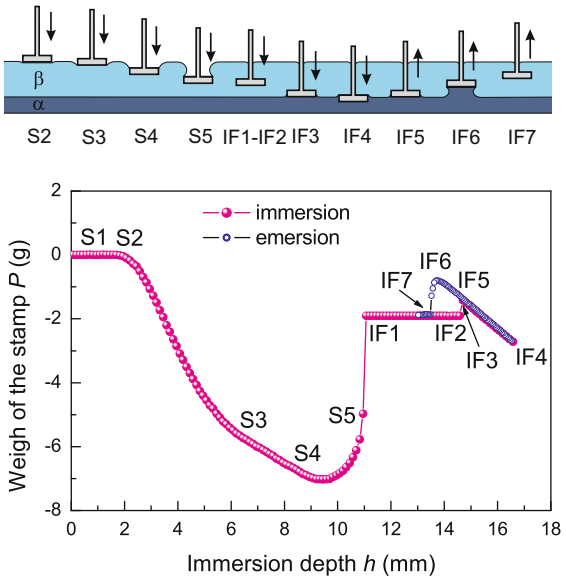

Fig. 1. Main stages of the measuring process and the experimental curve for liquid $Al_{64}In_{36}$ at 923 K. S5 is the point where the stamp gets fully immersed inside the less dense Al-rich liquid. At IF3 the stamp touches the denser In-rich liquid. At IF4 the stamp motion is reversed.

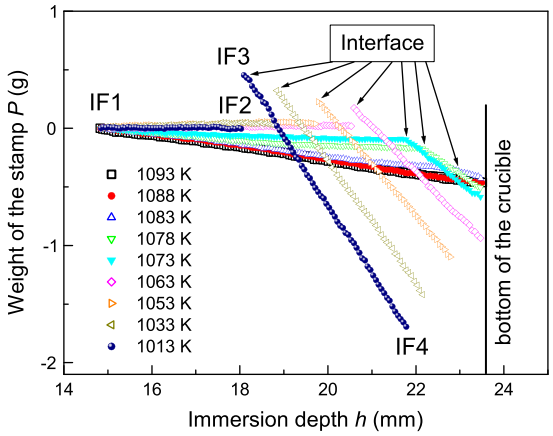

Fig. 2. Variation of the weight of the stamp (P) as a function of its immersion depth (h) into the liquid $Al_{75}In_{25}$ at different temperatures. The curve $P(h)$ is linear at temperatures above 1088 K where the alloy is homogeneous. The slope of $P(h)$ changes at 1083 K due to the liquid demixing. As temperature decreases, the interface shifts closer to the surface due to increasing volume of the In-rich phase. The jump on the experimental curves (stages IF2–IF3) at temperatures below 1073 K is due to the wetting of Al-rich liquid by In-rich liquid at the presence of Al_2O_3 stamp.

coexist, the curves display two features: (i) a jump when the stamp meets the interface between the two liquids (stages IF2–IF3 in Figs. 1 and 2), and (ii) once the meniscus has formed, a change of the buoyancy force because of the density difference between the Al-rich and In-rich liquids, which is reflected in the change of the slope on the $P(h)$ curve. At temperatures above the binodal line, where the $Al_{75}In_{25}$ liquid is homogeneous (>1088 K), the $P(h)$ curve keeps a constant slope after the point IF1. Hence, the phase separation temperature can be determined directly from the shape of the $P(h)$ curve.

The ST of Al–In binary liquid alloys was measured for nine compositions ranging from 4.7 to 88.5 at.% In. For each alloy, 1153 K was always the first temperature at which the measurements were performed, after homogenization for 8 h. Then, successive measurements were carried out at lower temperatures, stepped every 10 or 20 K down to the temperature where the sample solidifies. Both the single-liquid and two-liquid regions were investigated. The binodal temperature of each alloy could be determined from these series of experiments, as explained above. The ST of pure In was measured between 443 and 1073 K. The liquid–liquid IFT of the $Al_{64}In_{36}$ alloy could be measured between 913 and 1073 K, a temperature range which covers almost the whole miscibility gap because the investigated alloy is close to the critical composition.

The $P(h)$ curves were acquired in a tensiometer apparatus consisting of a vertical cylindrical chamber, a heating system, an electronic balance and a device enabling precise vertical displacement of the crucible containing the alloy. Details on the tensiometer can be found elsewhere [6,7,19,23,24].

The Al–In alloys were prepared from high purity (99.999%) Al and In. Before heating, the chamber was evacuated to a residual pressure of less than 5×10^{-6} mbar and then filled with a gas mixture of Ar–10H_2 (vol.%) with a total pressure of about 1 bar. A niobium getter was used to achieve a low oxygen partial pressure into the chamber during the measurements. The force exerted on the stamp was measured with an accuracy of $\pm 10^{-5}$ N. The relative error on density and density difference is estimated to be 3%. The errors on the measurements of surface and interfacial tension are of about 5%.

The phase transformations of the $Al_{75}In_{25}$ and $Al_{64}In_{36}$ alloys were also studied by differential scanning calorimetry (DSC) using a NETZSCH DSC 404C instrument. The temperature was calibrated on the melting points of 99.999% pure metals (Ag, Al, Bi, Cu, In, Si, Sn). Several samples of about 170 mg were prepared by arc melting under an atmosphere of argon after evacuating the furnace down to 10^{-3} mbar. The samples chosen for the measurements had lost less than 2 mg. They were processed in the DSC in alumina crucibles under an argon flow with heating and cooling rates of 20 K min^{-1}. Three runs were performed on each sample. The overall uncertainty of the DSC measurements was estimated to be less than ±3 K.

Temperature–time curves were also recorded for the Al–In samples processed in the tensiometer during heating/cooling with a rate of 1 K min^{-1} as in conventional thermal analysis. The sample temperature was measured with ±3 K of accuracy by means of the thermocouple inserted into a bore in the bottom of the sample crucible.

Several $Al_{64}In_{36}$ alloys solidified at 1 K min^{-1} in graphite crucibles were also examined by a FEI NOVA NANO SEM 200 scanning electron microscope equipped with an energy dispersive X-ray (EDX) spectrometer. Before observation, the samples were cut, ground and polished to down to 1 μm with a diamond paste.

3. Results and discussion

3.1. Differential scanning calorimetry and thermal analysis

The DSC curves for the $Al_{75}In_{25}$ and $Al_{64}In_{36}$ alloys are plotted in Fig. 3. On heating $Al_{64}In_{36}$, the thin curve presents the first endothermic signal (onset at 432 K), which corresponds to the eutectic reaction. The second endothermic peak (onset at 912 K) corresponds to the monotectic transformation. After this peak, the alloy consists of two liquids, which mix upon further heating above the critical temperature T_C. As the thermal signal is small and diffuse, this temperature cannot be determined unambiguously. On cooling, the $Al_{64}In_{36}$ melt (thick line) separates into two liquids at 1087 K. We found that, for a given composition, demixing occurs always at the same temperature, as shown by Curiotto et al. for Cu–Co alloys [31]. Upon further cooling, the Al-rich phase solidifies according to the monotectic reaction, then the In-rich liquid phase left solidifies (onset at 892 K) according to a eutectic reaction (onset at 422 K). The temperature hysteresis found for a given phase transition during heating and cooling is explained by rather high heating/cooling rate (20 K min^{-1}). It is also probable

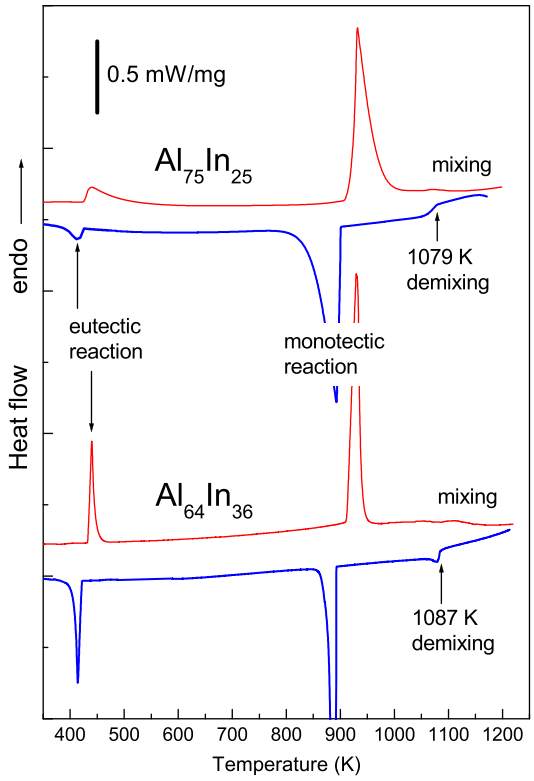

Fig. 3. DSC curves obtained with heating and cooling rate of 20 K min^{-1}. On heating (thin lines), the two alloys have a eutectic transformation followed by the monotectic reaction. The mixing signal is small and diffuse. Upon cooling (thick lines), liquid demixing occurs at the binodal temperature; for a given composition, this temperature is always the same. On further cooling the sample solidifies following the monotectic and the eutectic reactions.

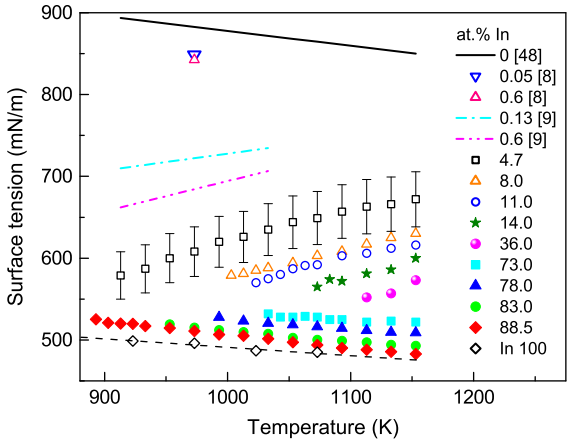

Fig. 4. Temperature dependence of the surface tension of the Al–In liquid alloys outside the liquid–liquid miscibility gap. For the sake of clarity, the experimental uncertainty of 5% is shown only for the 4.7 at.% In alloy.

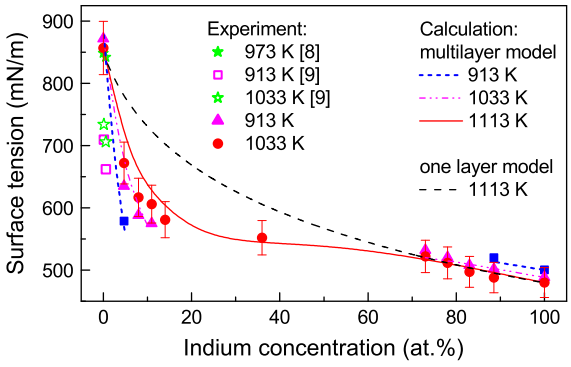

Fig. 5. Isothermal composition dependence of the surface tension in the Al–In liquid alloys outside the liquid–liquid miscibility gap.

that the temperature of solidification reactions somewhat decreases at high cooling rate due to undercooling. The hysteresis disappeared when the thermal-analysis data were obtained with a lower heating/cooling rate of 1 K min^{-1}.

Within the experimental error, the temperatures of the eutectic and monotectic reactions are identical for $Al_{75}In_{25}$ and $Al_{64}In_{36}$, but the demixing temperature is higher for $Al_{64}In_{36}$ (1079 K and 1087 K, respectively), showing that this alloy is closer to the critical composition. The eutectic and monotectic temperatures obtained with conventional thermal analysis are consistent with those obtained in the DSC study. These results will be shown and discussed in Section 3.4, related to the Al–In phase diagram.

3.2. Surface and interfacial tensions as a function of temperature

The temperature and composition dependences of the surface tension of the Al–In alloys are presented in Figs. 4 and 5 respectively. For each alloy, the ST values are reported from 1153 K down to the temperature of the miscibility gap. The ST values for three alloys with 0.05, 0.13 and 0.6 at.% In taken from Refs. [8,9] are also plotted for comparison.

The binodal temperatures were detected by three means: (1) thermal analysis, (2) the change of density when the (l–l) interface is crossed, and (3) a jump in the $P(h)$ tensiometric curve due to the formation of an interfacial meniscus on the stamp. Close to the critical temperature, where the top of the gap is very flat and the IFT is very small, the second method is the most efficient for detecting the location of the binodal line. During our ST or IFT measurements, liquid sample is kept at a constant temperature for relatively long time (one run takes about 20–30 min). The IFT between the two liquid phases is the parameter delaying the liquid separation and it is very low (see later in this section). Calculations on the liquid phase separation in similar immiscible liquids ([31]) show that the nucleation rate of liquid demixing with undercooling below 1 K is in the order of 10^{33} nuclei m^3 s^{-1}. Thus it is quite improbable that a homogeneous undercooled melt persists during the experiment. The absence of undercooling of the liquid demixing in macroscopic samples was also confirmed by Uebber and Ratke [32], who could undercool a Zn–Pb melt only by gas atomization.

The critical temperature T_C can also be estimated from the temperature dependence (i) of the IFT and (ii) of the

difference in densities of the coexisting liquid phases. Both quantities obey a power law as the temperature approaches T_C with critical exponents equal to ~1.3 and ~0.3 respectively. This was experimentally demonstrated by Kaban and Hoyer [24].

In principle, the IFT can be measured for any alloy of composition lying within the miscibility gap. However, because T_C will be determined from the fit of the experimental data, it is desirable to use an alloy, which is demixed in the largest temperature interval. For this reason, we have chosen the $Al_{64}In_{36}$ composition, which is supposed to correspond to the critical composition or at least to be close to it, according to various experimental observations and thermodynamic calculations presented in the next section.

The temperature dependence of the IFT for $Al_{64}In_{36}$ is plotted in Fig. 6. These data agree very well with those reported by Merkwitz and Hoyer [7]. The fit with the power law $\sigma_{L1L2} = \sigma_0 \cdot (1 - T/T_C)^{1.3}$ yields to a critical temperature $T_C = 1086 \pm 6$ K and a constant $\sigma_0 = 315 \pm 4$ mN m^{-1} (Fig. 6).

3.3. Density of coexisting liquid phases as a function of temperature

Fig. 7 shows the densities of the Al-rich and In-rich liquids determined from the tensiometric curves for the $Al_{64}In_{36}$ alloy as detailed in Ref. [30]. The experimental values are compared with the theoretical densities computed with the ideal solution approximation, i.e. assuming that there is no excess volume upon mixing of liquid Al and In. The molar volumes of pure Al and In were taken from Ref. [33] and the compositions of coexisting liquids were extracted from the phase diagram of Sommer et al. [34] and from our optimized phase diagram described in the next section. The agreement is good in the middle of the miscibility gap. The largest discrepancies between the experimental and calculated densities are for the alloys close to the monotectic and the critical temperature (up to about 7% if our phase equilibrium data are used). The difference could be due to deviations from the ideal solution approximation. However, it should also be noted that the experimental error on the density of coexisting liquids might be larger than the uncertainty of 3% estimated mathematically [6,30,35].

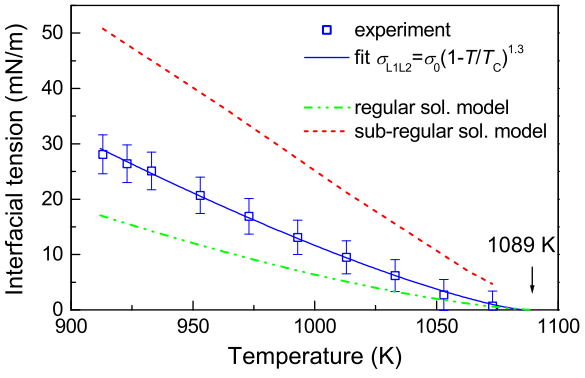

Fig. 6. Liquid–liquid interfacial tension in the Al–In system: symbols – experiment; solid line – fit with the function $\sigma_{L1L2} = \sigma_0 \cdot (1 - T/T_C)^{1.3}$; dash-dot-dot line – calculation with the regular solution model; dash line – calculation with the sub-regular solution model.

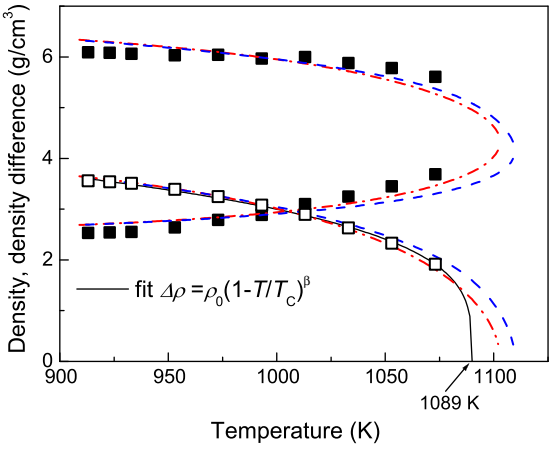

Fig. 7. Temperature dependence of the density and density difference in liquid $Al_{64}In_{36}$ alloy: symbols – experimental values (the experimental error is comparable with the size of symbols); full squares – density of the two coexisting liquids; empty squares – difference of the density of the two coexisting liquids; dash line – theoretical values obtained with the compositions from the phase diagram of Sommer et al. [34]; dash-dot-line – theoretical values obtained with the phase compositions from our optimization; full line – fit of the experimental density difference with the function $\Delta\rho = \rho_0 \cdot (1 - T/T_C)^\beta$ (parameters obtained from the fit: $\rho_0 = 5.88 \pm 0.17$, $T_C = 1089 \pm 4$ K, $\beta = 0.27 \pm 0.02$).

The calculated density difference is also shown in Fig. 7. In the temperature range between 913 K and about 1050 K, there is excellent agreement with our present results as well as with the experimental data reported earlier by Merkwitz and Hoyer [7]. The difference between experiments and calculations at higher temperature are due to (i) the experimental error, (ii) the ideal solution approximation, and (iii) the uncertainty of the compositions of coexisting phases (see next section).

The fit of our experimental density difference using the power function $\Delta\rho = \rho_0 \cdot (1 - T/T_C)^\beta$ yields to a critical temperature $T_C = 1089 \pm 4$ K, a critical exponent $\beta = 0.27 \pm 0.02$, and a constant $\rho_0 = 5.88 \pm 0.17$ g cm^{-3}.

3.4. Miscibility gap and bulk thermodynamics

Phase equilibria in the Al–In monotectic system have been extensively investigated [34,36–43]. Whereas the phase diagram is well established in the solid state, there are serious discrepancies on the location of the liquid–liquid miscibility gap, particularly close to the critical point. The monotectic compositions were reported to range from (4.0–6.0) to (87–89) at.% In at a monotectic temperature of 910–913 K. The values reported for the critical temperature span between 1088 and 1248 K [34,36–43].

Fig. 8 compares experiments and calculations of the Al–In phase diagram. The phase diagram fitted by Sommer

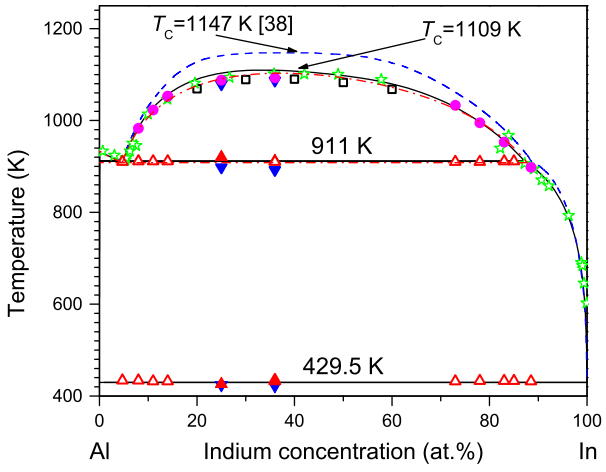

Fig. 8. Al–In phase diagram: full line – thermodynamic calculation of Sommer et al. [34]; dash line – thermodynamic calculation of Murray [38]; dash-dot line – thermodynamic calculation performed in the present work. Symbols – experimental data: stars – thermal analysis of Predel [37]; squares – viscosity measurements of Herwig and Hoyer [43]; open triangles – DTA (1 K min^{-1} heating rate), this work; closed triangles – DSC (20 K min^{-1} heating/cooling rate), this work; closed circles – tensiometry, this work.

et al. [34] agrees much better than that of Murray [38] with our experimental data and with the values reported by Predel [37] and by Herwig and Hoyer [43].

It is noteworthy to discuss the results obtained on $Al_{11.5}In_{88.5}$. By tensiometric measurements, we have found that this alloy was liquid and homogeneous down to 898 K. This temperature coincides with the DSC value reported by Predel [37] and with the liquidus line on the phase diagram of Sommer et al. [34]. However, the phase diagram of Murray [38] shows that this alloy should be at the In-rich limit of the miscibility gap at the monotectic temperature $T_M = 911$ K.

The phase diagram of Sommer et al. [34] proposes the best thermodynamic fit of both the liquid–liquid and the liquid–solid equilibria in the Al–In monotectic system. The corresponding Gibbs free energy of the liquid phase is modelled with four Redlich–Kister parameters [44], three of them being temperature dependent. In order to use the sub-regular multilayer model for calculating the surface and interfacial tension [22] (presented in Section 3.5), we have recalculated the Gibbs free energy for the Al–In liquid phase using only two Redlich–Kister parameters. The excess Gibbs free energy in our optimization is expressed as:

$$\Delta G^{XS} = x_{Al}x_{In}[L_0 + L_1(x_{Al} - x_{In})] \quad (1)$$

where x_{Al} and x_{In} are the mole fractions of Al and In, and the two parameters L_0 and L_1 are:

$$L_0 = -10267 + 85.651 \cdot T - 0.05533 \cdot T^2 \quad (2)$$

$$L_1 = 8787 - 12.017 \cdot T + 0.0066 \cdot T^2 \quad (3)$$

T is the temperature in Kelvin.

The phase diagram computed with this new fit for the Gibbs free energy of the liquid phase is shown in Fig. 8. We did not re-optimize the solid phases. Our calculations fit well the experimental data as far as the miscibility gap is concerned.

3.5. Surface tension and interfacial tension calculations

Modelling of the prewetting and complete wetting phenomena in liquid alloys requires a correct description of the chemical gradient at surfaces and interfaces. The model of Butler [45] supposes that the surface (interface) is a separate phase of composition different from that of the bulk. This simple description does not agree with the Gibbs adsorption equation because it constraints the surface composition gradient into the equivalent of one atomic monolayer [18]. Butler's model calculates reasonable values of ST in miscible systems; however, it gives systematically higher values for systems with a surface concentration gradient which spreads into several layers, like the monotectic Al–In alloys [46]. Wynblatt et al. [18] developed a multilayer model, which allows calculation of ST and IFT for liquid surfaces and (l–l) interfaces based on the regular solution approximation. However, such approximation supposes that the miscibility gap of the binary system is symmetrical about the equiatomic composition, while real monotectic systems have, like Al–In, an asymmetrical binodal line. Antion and Chatain [22] improved the multilayer model in order to take into account the asymmetry of the miscibility gaps by describing the Gibbs free energy with the sub-regular solution approximation. The code can be found at the electronic address [47]. In what follows, we compare the ST and IFT calculated with this model with our experimental results and then we use the model to estimate the wetting temperature in the Al–In system.

The calculations require the input of two bulk energy parameters (L_0 and L_1, see Eqs. (2) and (3) in Section 3.2), the surface tensions of pure liquid Al ($\sigma_{Al} = (1060 - 0.182\ T)$ mN m^{-1} [48]) and In ($\sigma_{In} = (594 - 0.103\ T)$ mN m^{-1}, this work), and the molar surface (interfacial) area. We estimate this last parameter by averaging the molar areas of pure In and pure Al. For each component i with the molar volume V_i the molar area $\Omega_m(i)$ is calculated with the expression:

$$\Omega_m(i) = f \cdot N_A^{\frac{1}{3}} \cdot V_i^{\frac{2}{3}} \quad (4)$$

where N_A is the Avogadro's number and f is the factor of two-dimensional density, which equals to 1.091 for a (1 1 1) plane of the face-centred-cubic lattice. It is assumed that at liquid surfaces and liquid/liquid interface the liquid layers have such a density [49,18]. The molar volumes of pure Al and In were those used for density calculations (Section 3.2) [33]. The average molar area at 913 K is found to be equal to 54,000 m^2 mol^{-1}. The number of layers in which the compositional gradient at the surface (or at the interface) spreads has to be chosen carefully: the more confined the gradient, the larger the calculated ST or IFT. We chose an optimum number of layers such that an additional layer leads to a decrease of the ST or IFT of less than 0.1%.

In Fig. 5 the surface tension calculated for different alloys at three temperatures (913 K, 1033 K and 1113 K) on both sides of the miscibility gap is compared to the experimental data. The discrepancy is less than the experimental uncertainty of 5% for all compositions, except the region of small In concentrations where the difference is about 7.5%. The calculations reproduce well (i) the decrease of ST as a function of the In concentration, and (ii) the increase of the ST of the Al-rich alloys, at a constant composition as a function of temperature. A positive slope of the ST against temperature is related to the desorption of In from the Al surface as temperature increases. Such behaviour is usual for immiscible alloys which contain a low level of the segregating component. It has been already observed for Ga-rich Ga–Pb alloys [50] and explained in Ref. [18].

For comparison, the Al–In ST at 1113 K, calculated using Butler's model [45] as described in Ref. [46], is reported in Fig. 5. It is seen that this monolayer model gives too high ST values.

In Fig. 6 the calculated (*l*–*l*) IFT curve is compared with the experimental data. It is important to mention that the IFT strongly depends on the difference in composition between the two coexisting liquids. Using the previous version of the multilayer model, where the interactions in the liquid were described within a regular solution approximation, Merkwitz et al. [6,7] found that the IFT in binary monotectic alloys is 1.5–1.6 times less than the respective experimental data. The main reason for such underestimate is that the calculated miscibility gap, which fits the experimental critical temperature with the regular solution approximation, is systematically narrower than a real miscibility gap. The sub-regular version of the multilayer model [22] uses as input the correct compositions of the coexisting liquids but predicts IFT values of 3–20 mN m^{-1} (about 1.8 times) higher than the experimental data. We conclude that the accuracy of the estimate of both the IFT and the ST ranges within a few tens of mN m^{-1}. This error has relatively larger impact on the IFT than on the ST which is of the order of 10 times larger than the IFT.

The surface composition profiles shown in Fig. 9, calculated with the sub-regular multilayer model for two different alloys, give further insights into the behaviour of the In adsorption at the surface. Fig. 9a shows the surface composition gradient of an Al-rich alloy containing 0.6% In in the five layers at the surface. In the temperature range between 913 and 1200 K the In adsorption remains confined within the first two atomic layers and the composition gradient is steep. As temperature increases, In adsorption decreases. However, as shown in Fig. 9b, for the $Al_{64}In_{36}$ alloy whose composition lies close to the critical composition, the concentration gradient at the surface flattens and spreads within a large number of layers. For such alloy, when the temperature increases, the In adsorption decreases by reducing the spreading of the compositional gradient.

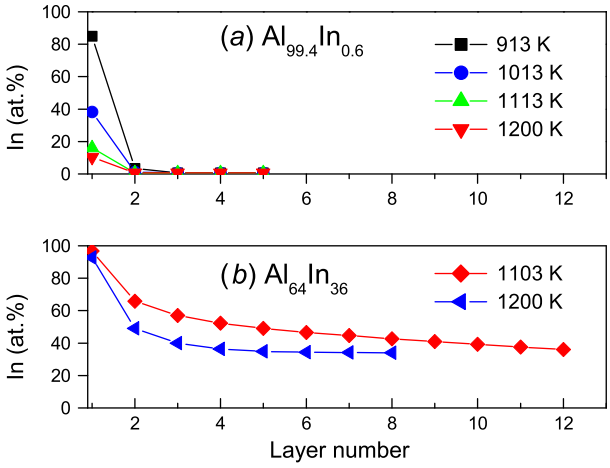

Fig. 9. Concentration profiles at the surface: (a) $Al_{99.4}In_{0.6}$; (b) $Al_{64}In_{36}$. The lower the temperature, the higher the In adsorption. More than twelve layers are required for a correct description of the concentration profile from the surface to the bulk in liquid $Al_{64}In_{36}$ near the critical temperature.

3.6. Complete wetting, segregation and microstructure of solidification

After solidification, a thick layer of In has been observed by eye at the free surface of all the samples which have been used for measuring the ST and IFT. This suggests that complete wetting stands in the whole region where the Al–In miscibility gap is stable. We have compared the IFT with the difference of ST of the Al-rich and In-rich phases, extrapolated on the binodal line. Within the experimental error on the ST and IFT values, this difference is of order of the IFT measured over the whole miscibility gap. This suggests that the Al-rich liquid is perfectly wetted by the In-rich liquid already at the monotectic temperature.

The wetting transition can be estimated using the multilayer model. As shown in Ref. [14], T_W is the temperature where the prewetting line meets the liquid miscibility gap. The prewetting line is the location of the temperature where the first surface layer undergoes a first order transition. Fig. 10 shows the prewetting line calculated for Al–In with the multilayer model. The two lines are getting closer at lower temperature but never meet, which suggests that complete wetting stands at all temperatures.

Experiments attempting to measure the effect of gravity on the thickness of the wetting layer were performed with the $Al_{64}In_{36}$ alloy whose composition is close to the critical one. Several samples were heated at 1 K min^{-1} up to 1153 K, homogenized, and cooled down to room temperature slowly (rate less than 1 K min^{-1}). Keeping the volume of the alloy constant and varying the diameter of the carbon crucible in which the alloy is contained, the height of the Al-rich phase was tuned. After solidification, all samples displayed In-rich wetting layers at their free surfaces and at the wall with the crucible: the Al-rich phase is encapsulated by a wetting layer, as shown in Fig. 11 on EDX images of the section of $Al_{64}In_{36}$ samples. A film of almost

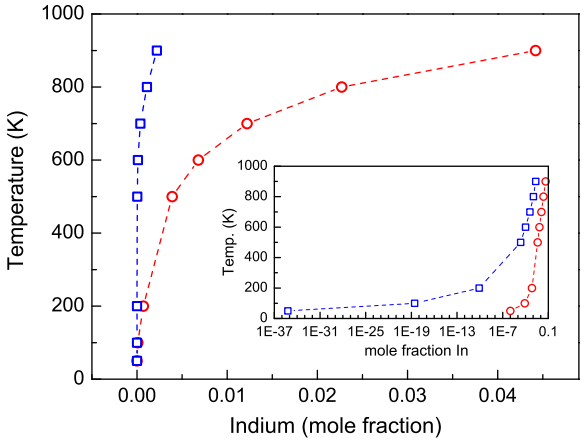

Fig. 10. Prewetting (squares) and binodal (circles) lines in the Al–In monotectic system. The two curves get closer when the temperature decreases, but they do not cross. This is highlighted in the insert where *x*-axis is in logarithmic scale.

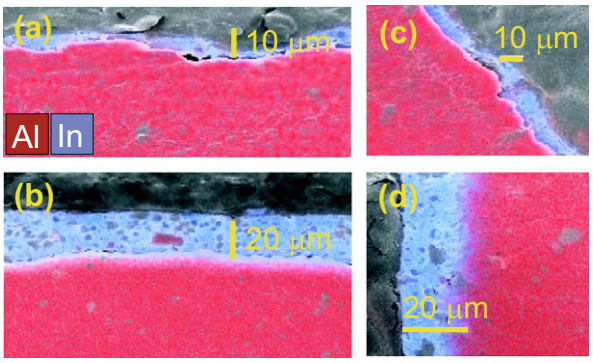

Fig. 11. EDX images of sections of the $Al_{64}In_{36}$ samples showing the In-rich wetting layer: (a) at the free surface of a sample whose Al-rich phase height is about 33 mm; (b) at the free surface of a sample whose Al-rich phase height is about 10 mm; (c) at the crucible wall, at a distance from the Al-rich/In-rich interface of about 31 mm; (d) at the crucible wall, at a distance from the Al-rich/In-rich interface of about 8 mm.

pure In encapsulates the Al-rich phase. The In-rich wetting layer thickness decreases with the increase of the Al-rich phase height: it is about 5–6 μm when the height of the Al-rich phase reaches 33 mm (Fig. 11a and c) and 22–25 μm when the height of the Al-rich phase is about 10 mm (Fig. 11b and d). The same thickness of the In-rich layer is measured at the free surface of the alloy or at the crucible wall (Fig. 11c and d) and it depends only on the height of the Al-rich phase.

The thickness found for the wetting layer is of the order of few microns. In other monotectic alloys (Ga–Bi [51], Cu–Fe [52], Cu–Co [53] and Ga–Pb [54]), micron thick wetting layers have also been observed. This is much larger than any wetting layer measured at equilibrium in organic liquids [20]. However, in the paper of Moldover and Cahn [11] a macroscopic thick layer has been reported. As noticed by Widom [21], such a large thickness can actually be found when demixing occurs close to the critical temperature because the coherence length of composition fluctuations is of the order of hundreds of nanometers there. But the thicknesses we have measured are much too large to be interpreted by the model of Widom [21] or that of de Gennes [55].

We think that both above and below the monotectic temperature, complete wetting actually stands in Al–In. However, the thickness of the In-rich layer we observe at the surface and at the interface of the solidified $Al_{64}In_{36}$ samples (Fig. 11) is related to the macroscopic segregation of In due to the decreasing solubility of In in solid Al upon cooling. Indeed, the In solubility decreases by about a factor of 10^2 by cooling Al–In from the monotectic temperature down to 573 K [56]. Recently, it has been observed that the surface of diluted Al-rich solid alloys (Al–In, Al–Bi, Al–Pb) is significantly enriched by the low ST metal (In, Bi and Pb, respectively) after heat treatment at about 50–100 K below the monotectic temperature. Either droplets with diameter of several microns [57] or layers up to 0.2 μm thick [58] were measured. In the Al–Bi foils containing 50–1000 wt. ppm of Bi, the surface region was found to contain up to 13–25% of all the Bi available in the foil. In our $Al_{64}In_{36}$ samples, the In content of the solid Al-rich phase is rather large and the cooling time from the monotectic to room temperature is long. Therefore, a large quantity of In can segregate to the free surface and to the interface with the wall and thicken the wetting layer which was already formed above the monotectic temperature.

4. Conclusions

We have performed a detailed experimental study on both the surface energetics and the bulk thermodynamics of Al–In monotectic alloys. We have shown that a technique derived from the Wilhelmy method frequently used to determine the surface tension and density of liquids can also be utilized to locate the liquid miscibility gap and the wetting transition, which takes place in monotectic alloys. The consistent set of surface, interfacial and bulk data acquired on Al–In was then analysed using a sub-regular solution model from which the wetting temperature could be estimated to lie well below the eutectic temperature of the Al–In system. This estimate of the location of the wetting transition is consistent with the observation of a wetting In-rich film both at the surface of Al-rich alloys and at its interface with the wall of the graphite crucible which contains the alloys. However, while the thickness of the film depends on gravity, it is too thick (microns) to be related only to the wetting phenomenon. We suggest that the film thickness is also driven by solid-state transformations which take place below the monotectic temperature during the cooling of the samples down to room temperature.

Acknowledgments

This study has been supported by the German Research Foundation (DFG). Prof. Rainer Schmid–Fetzer and

Dr. Joachim Gröbner are gratefully acknowledged for the discussions and valuable information on the phase equilibria in monotectic systems. We are indebted to Mr. Torsten Jagemann for the help with EDX analysis. Mr. Rene Krone is acknowledged for his technical assistance.

References

[1] Cahn JW. Metall Trans 1979;10A:119.
[2] Zhao J, Ratke L, Jia J, Li Q. J Mater Sci Technol 2002;18:197.
[3] Christian JW. The theory of phase transformations in metals and alloys. Oxford: Pergamon Press; 1965.
[4] Young NO, Goldstein JS, Block MJ. J Fluid Mech 1959;6:350.
[5] Martin-Garin L, Dinet A, Hicter JM. Mémoir Etudes Scie Rev Métall 1981;5:269.
[6] Merkwitz M. Ph.D. thesis, TU Chemnitz; 1997. <http://archiv.tu-chemnitz.de/pub/1997/0036/index.html>.
[7] Merkwitz M, Hoyer W. Z Metallkd 1999;90:363.
[8] Lang G. Aluminium 1973;49:231.
[9] Alchagirov BB, Chochaeva AM, Bekulov VB, Khokonov KB. High Temp 2003;41:472.
[10] Cahn JW. J Chem Phys 1977;66:3667.
[11] Moldover MR, Cahn JW. Science 1980;207:1073.
[12] Chatain D, Wynblatt P. Surf Sci 1996;345:85.
[13] Tostmann H, DiMasi E, Shpyrko OG, Pershan PS, Ocko BM, Deutsch M. Phys Rev Lett 2000;84:4385.
[14] Shim H, Chatain D, Wynblatt P. Surf Sci 1998;415:346.
[15] Shim H, Chatain D, Wynblatt P. Surf Sci 2001;476:L273.
[16] Shim H, Chatain D, Wynblatt P. Surf Sci 2000;465:97.
[17] Nattland D, Poh PD, Freyland W. J Phys Condens Matter 1995;7:L457.
[18] Wynblatt P, Saul A, Chatain D. Acta Mater 1998;46:2337.
[19] Hoyer W, Kaban IG. In: Herlach DM, editor. Phase transformations in multi-component melts. Weinheim, Germany: J. Wiley-VCH; 2008. p. 19–38.
[20] Bonn D, Ross D. Rep Prog Phys 2001;64:1085.
[21] Widom B. J Chem Phys 1975;62:1332.
[22] Antion C, Chatain D. Surf Sci 2007;601:2232.
[23] Kaban I, Mhiaoui S, Hoyer W, Gasser JG. J Phys Condens Matter 2005;17:7867.
[24] Kaban IG, Hoyer W. Phys Rev B 2008;77:125426.
[25] Wilhelmy L. Ann Phys 1863;119:177.
[26] Young T. Philos Trans Roy Soc Lond 1805;95:65.
[27] De Laplace PS. Sur l'Action Capillaire. Suppl to Book 10 Traité de Mécanique Céleste. Paris; 1806.
[28] Schulze HJ. In: Fuerstenau DW, editor. Developments in mineral processing. vol. 4. Amsterdam: Elsevier; 1984. p. 52–154.
[29] Keller JB. Phys Fluids 1998;10:3009.
[30] Mirković D, Gröbner J, Kaban I, Hoyer W, Schmid-Fetzer R. Int J Mater Res 2009;100:176.
[31] Curiotto S, Pryds NH, Johnson E, Battezzati L. Metall Mater Trans A 2006;37:2361.
[32] Uebber N, Ratke L. Scripta Metall Mater 1991;25:1133.
[33] Iida T, Guthrie RIL. The physical properties of liquid metals. Oxford (UK): Clarendon Press; 1993.
[34] Sommer F, Krull HG, Yu SK. In: Ratke L, editor. Immiscible liquid metals and organics. Oberursel, Germany: DGM Informationsgesellschaft; 1993.
[35] Kaban I, Gröbner J, Hoyer W, Schmid-Fetzer R. J Mater Sci 2010;45:2030, doi:10.1007/s10853-009-3713-3.
[36] Campbell AN, Buchanan LB, Kuzmak JM, Tuxworth RH. J Am Chem Soc 1952;74:1962.
[37] Predel B. Z Metallkd 1965;56:791.
[38] Murray JL. Bull Alloy Phase Diagrams 1983;4:271.
[39] Kim SS, Sanders Jr TH. Model Simulat Mater Sci Eng 2006;14:1181.
[40] Ansara I, Bros JP, Girard C. Calphad 1978;2:187.
[41] Sharma RC, Srivastava M. Calphad 1992;16:409.
[42] Hultgren R, Desai PD, Hawkins DT, Gleiser M, Kelley KK. Selected values of the thermodynamic properties of binary alloys. In: Francisco S, editor. California: Jossey-Bass Publishers; 1981.
[43] Herwig F, Hoyer W. Mater Sci Eng A 1995;190:L5.
[44] Redlich O, Kister AT. Ind Eng Chem 1948;40:345.
[45] Butler J. Proc Roy Soc A 1935;135:348.
[46] Brillo J, Chatain D, Egry I. Int J Mater Res 2009;100:53.
[47] <http://www.cinam.univ-mrs.fr/cinam/spip.php.>?article160 – if you use this code, please cite refs. 22 and 18.
[48] Keene B. Int Mater Rev 1993;38:157.
[49] Faber TE. Introduction to the theory of liquid metals. Cambridge (UK): University Press; 1972.
[50] Serre C, Wynblatt P, Chatain D. Surf Sci 1998;415:336.
[51] Perepezko JH, Galaup C, Cooper KP. Mater Res Soc Symp Proc 1982;9:491.
[52] Wilde G, Perepezko JH. Acta Mater 1999;47:3009.
[53] Curiotto S, Battezzati L, Johnson E, Pryds N. Acta Mater 2007;55:642.
[54] Calmes C, Giuranno D, Chatain D. J Mater Sci 2009;44:5949.
[55] De Gennes PG. J Phys Lett 1981;42:377.
[56] Kemerink GJ, Pleiter E, Kruithof GH. Hyperfine Interact 1987;35:619.
[57] Ashitaka Z, Thompson GE, Skeldon P, Habazaki H, Shimizu K. J Mater Sci 2001;36:2237.
[58] Gundersen JTB, Aytac A, Nordlien JH, Nisancıoglu K. Corros Sci 2004;46:697.